This is a repository copy of *Catalytic conversion of toluene over a biochar bed under an inert atmosphere – The comparison of chars from different types of wood and the role of selected metals*.

White Rose Research Online URL for this paper:
http://eprints.whiterose.ac.uk/163233/

Version: Published Version
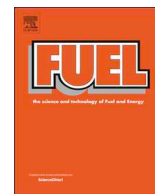
**Article:**

Full Length Article

# Catalytic conversion of toluene over a biochar bed under an inert atmosphere – The comparison of chars from different types of wood and the role of selected metals

Agnieszka Korus[a,b,*], Abby Samson[c], Andrzej Szlęk[a]

[a] Department of Thermal Technology, Silesian University of Technology, Gliwice, Poland
[b] School of Engineering, University of Lincoln, Lincoln, UK
[c] Department of Mechanical Engineering, University of Sheffield, Sheffield, UK

ABSTRACT

In this paper, toluene, a tar-representing compound, was used in pyrolytic conversion tests with a wood-derived char catalyst. The decomposition mainly occurred via two competing heterogeneous reactions; the favoured reaction led to coke formation on the catalyst bed. With char saturation of the carbon deposit, a second demethylation reaction gained significance, until selectivity towards benzene formation reached 12–16%. By-products of the secondary reaction (xylenes, ethylbenzene and styrene) were also detected; however, no gas-phase toluene decomposition occurred. The principles of toluene conversion were the same for all of the examined chars from the different tree species. However, a quantitative difference was observed between the chars from the wood from coniferous and deciduous trees. Pine yielded char with less mesopores and active sites and thus demonstrated a lower efficiency as a catalyst for toluene decomposition. An assessment of alkali and alkaline earth metals importance revealed that, while their presence in the char strongly enhances its oxidation rate, they did not affect the toluene pyrolysis.

## 1. Introduction

Catalytic conversion of aromatic hydrocarbons is an important process that has a wide range of applications in the chemical industry as well as energy production, e.g. for tar removal from syngas. A number of natural minerals and synthetic catalysts can be used for this purpose; transition metal-based materials proved to be highly effective [1], yet they get poisoned easily and their regeneration is expensive [2]. Biomass-derived char is a promising alternative to commercial catalysts, as it can be produced *in situ* in a gasifier, which means that it is a low-cost and easily accessible material. It is also generally acknowledged that, amongst typical biomass types, woody feedstock yields char with the best catalytic properties [2–4]. However, due to the heterogeneous nature of tar, as well as the non-uniform structure of biochars, fundamental experiments under simplified conditions are required to achieve a better understanding of the tar-char interaction. In the literature, a single compound was often selected to represent tar from gasification [5–9]. Lighter aromatics, such as toluene or naphthalene, have often been of interest, as their removal is more challenging, compared to the heavier and more abundantly substituted molecules [5]. Studies into

the catalytic conversion of hydrocarbons are often performed under isothermal conditions in the presence of a fixed bed of a catalytic material. Biochars from various feedstocks (wood, sewage sludge, nut shells, etc.) have been considered and both inert and reactive atmospheres, e.g. $N_2/H_2O$, $N_2/H_2O/H_2$ or $N_2/CO_2$, have been investigated [5–7,10].

A few characteristic phenomena are commonly observed during conversion studies of hydrocarbons. The formation of coke from the decomposition of aromatic compounds over the surface of a catalyst has been frequently reported [5–7]. This solid layer of carbon deactivates the catalytic material by covering its active sites as well as filling in and blocking its pores [2]. However, the heterogeneous decomposition of hydrocarbons into solid carbon is the main, most efficient conversion pathway, thus this process is necessary in order to maintain the high efficacy of the tar removal [11]. Most studies focused on reaching and preserving a high compound conversion rate by searching for chars with the best catalytic properties and introducing various methods to prolong their catalytic activity [5,6,9]. However, the conversion products, other than coke and gaseous species, have rarely been quantified. Mani et al. reported the formation of benzene during steam reforming

---

of toluene [12], but in general, the more detailed studies into the distribution of the products were aimed at tar formation rather than decomposition. Thus, thorough analyses of the products has been limited to more complex molecules such as eugenol or anisole [13,14].

The catalytic properties of char are usually attributed to the active sites that are dispersed on its surface, and to the development of this surface, i.e. the surface area and pore size distribution. Some of the active sites are represented by defined structures such as alkali and alkaline earth metals (AAEM) or O-containing functional groups, such as acidic lactols, lactones, phenolic and carboxylic groups or basic carbonyls and quinones [15,16]. Moreover, the carbonaceous matrix of char can itself act as a catalyst. The "unsaturated carbons", i.e. atoms with unpaired electrons, occur on the surface of a carbonaceous material due to defects in the carbon lattice. They are also created during the formation of char as a result of thermal decomposition of the feedstock structure [17]. Morphology is also important when estimating the catalytic properties of char; a well-developed surface area facilitates more active sites, while pore distribution determines their accessibility. Moliner et al. [18] reported that highly microporous structures are prone to being blocked by coke deposition at the narrow mouths of the pores. Thus, more mesoporous structures are often recommended for catalysing the conversion of hydrocarbons [6]. The distribution of pore size in char is greatly influenced by its preparation conditions. It is generally acknowledged that thermal activation with $CO_2$ creates char that is more microporous while steam favours the creation of mesopores [19,20]. Thus, maintaining uniform conditions during char synthesis is necessary if the investigation is aimed at comparing different feedstocks.

Although the catalytic effect of AAEM species on the gasification and oxidation of solid carbon is well known [21,22], their role in the conversion of hydrocarbons is debatable. Klinghoffer et al. [16] observed that removing the inorganics from char decreased its efficiency in catalysing the decomposition of methane, and Dufour et al. [17] reported that biochar ash plays a negligible role in methane reforming. Therefore, the importance of AAEM species during the conversion of methylated aromatic compounds with no O-heteroatoms cannot be unambiguously determined.

This research focused on the catalytic conversion of a methyl-substituted single-ring aromatic, i.e. toluene. Wood-derived biochars were used as suitable catalysts with a well-developed structure [8,9]. In order to account for the properties of various species of trees, three different woods (pine, alder and beech) were used to synthesise activated char following a uniform procedure. Therefore, any effects of varying the conditions of the preparation process could be eliminated, thus enabling a true comparison of the char feedstocks. The physicochemical properties of the chars, such as the AAEM content, the presence of surface functionalities and the development of the surface area, were examined and correlated with their catalytic performance. An analysis of the liquid products of the toluene conversion over a char bed allowed for the formulation of the main decomposition pathways. A comparison of the two toluene feeding modes, continuous and intermittent, reaffirmed the heterogeneous nature of the toluene conversion. Moreover, the modification of the AAEM species content in the char resulted in expected and significant differences in the oxidation kinetics of the char, yet no changes in the toluene conversion were observed as a result of the applied treatment.

## 2. Experimental methods

### 2.1. Feedstock and char preparation

Three diversified wood species were selected as the feedstock for char preparation. Pine (*Pinus sylvestris*) represented coniferous softwood (2420 N), while alder (*Alnus glutinosa*) and beech (*Fagus sylvatica*) were chosen as deciduous trees with different hardness values – 2890 N and 6460 N on the Janka scale, respectively [23].

Raw, bark and knot-free wood was oven dried at 105 ℃ and then milled and sieved to obtain a 250 – 1000 μm fraction. The activated char from the selected species was separately prepared in batches and then further subsampled for the toluene conversion experiments. The char preparation process was carried out in a quartz tube reactor (27 mm i.d.) in an electrical furnace. For each batch, 20 g of wood was heated up to 800 ℃ in a $N_2$ flow with an average heating rate of 47 K/min. The first step of the char preparation was a 60 min isothermal pyrolysis process. This was followed by an activation step, which was achieved by the introduction of 15.5 vol% of steam, carried out for 80 min at an isothermal temperature of 800 ℃. Then the prepared char was cooled down to ambient temperature in a $N_2$ flow and stored in a desiccator.

Additional tests that involved char with a modified content of alkali and alkaline earth metals (AAEM) were also performed. To this end, 5 g of the activated alder char was subsampled and demineralised by shaking it in 50 mL of a 2.0 M HCl solution for 24 h. The sample was then rinsed in distilled water and dried at 60 ℃, then a 2 g subsample was further impregnated with $Na^+$ by shaking it for 24 h in 50 mL of a 0.5 M solution of sodium acetate and dried at 60 ℃. As a result, two modified alder chars were obtained, one with decreased amount of inorganics and one with a high concentration of selected metal species.

### 2.2. Materials analysis

In order to assess the differences between the types of wood that were selected for char preparation, their composition and surface chemistry was examined. The elemental and proximate analyses of the feedstock were carried out according to the appropriate standards: PN-EN ISO 18122:2016-01 and PN-EN ISO 18123:2016-01 for ash and volatile matter determination, respectively; and PN-EN ISO 16948:2015-07 and PN-EN ISO 16994:2015-06 for C, H, N, S analyses. The cellulose, lignin, and extractives contents were determined according to the PN-92/P-50092 standard comprising: the Seifert method using acetylacetone, dioxane, and hydrochloric acid; the Tappi method with sulfuric acid; and Soxhlet extraction with ethanol, respectively. The amount of hemicellulose in the sample was calculated by subtracting the share of the cellulose from the holocellulose content analysed with sodium chlorite. Additionally, Attenuated Total Reflectance Fourier-Transform Infrared Spectroscopy (ATR-FTIR) was applied to evaluate the character of the functional groups in the constituents of the raw wood.

In order to assess the catalytic potential of the chars that were obtained from the selected trees, the physicochemical properties of the prepared materials were then analysed in addition to the main experiment where a char bed was used to catalyse the decomposition of the toluene. Examination of the chemical features of the chars involved analysis of the surface functional groups by the ATR-FTIR, a thermogravimetric analysis coupled with Fourier-Transform Infrared Spectroscopy (TGA-FTIR) and Boehm titration methods.

The ATR-FTIR spectra of the surfaces of both the wood and the char were acquired using a Perkin Elmer Spectrum 100 spectrometer with a Universal Attenuated Total Reflectance module (UATR) equipped with a germanium crystal. For each sample, an average of five repetitions was carried out; each repetition was performed with a 4 cm$^{-1}$ resolution and 32 scans of the 4000 – 700 cm$^{-1}$ region. A programmed temperature desorption of alder char was carried out as a TGA-FTIR analysis, which was performed with a Netzsch STA 409 LUXX thermogravimeter coupled, by means of a heated transfer line, with the Perkin Elmer Spectrum 100 spectrometer equipped with a RedShift accessory for analysis of gaseous samples. A 100 mg char sample was heated up to 1000 ℃ in a 30 mL/min. $N_2$ flow in a TGA, with a heating rate of 5 K/min. Simultaneously, the released gases, namely CO and $CO_2$, were analysed online at intervals of 8 s. Pyrolysis in the TGA provided a mass loss curve of each sample. The first derivative (DTG) of this curve was compared with the peaks of the gas evolution profiles.

Unfortunately, due to the poor resolution of the FTIR spectra, only qualitative information was obtained from this analysis. However, both the ATR-FTIR and TGA-FTIR analyses produced some insight into the nature of the presence of O-containing functional groups on the surface of the char. The distribution of the acidic sites was additionally determined with a set of Boehm titrations that were performed according to the procedure standardised by Goertzen et al. [24,25], following a char pre-treatment that was proposed by Tsechansky and Graber [26], which involved stepwise washing with an acid and a base and was applied to remove any mobile species, such as metal cations or labile organic carbon. A detailed description of the procedure can be found in the previous paper [27]. AAEM species are considered to be other types of active sites [28]. The sodium, potassium, calcium and magnesium content in the chars was analysed with a SpectrAA 880 Varian Atomic Absorption Spectrometer after sample digestion with $HNO_3$.

In order to assess the structural features of the char, $N_2$ adsorption at 77 K was performed with a Micromeritics TriStar II 3020 analyser. The samples were outgassed under $N_2$ flow, at 200 °C, for 24 h prior to the analysis. A BET model was applied to calculate the total surface area. Due to the microporous nature of the samples, only the relative pressures $p/p_0 < 0.2$ were taken into account. The area of the micropores was estimated by a t-Plot method, using the Harkins and Jura thickness equation.

Apart from their role as catalysts, chars themselves can undergo oxidation, e.g. during thermal activation with steam. Hence, in order to evaluate their reactivity during oxidation, the kinetic parameters were obtained from a thermogravimetric analysis using a Netzsch TG 209 F3 Tarsus instrument. A heating rate of 10 K/min and a 12 vol% concentration of $O_2$ in $N_2$ was applied. The activation energy and the pre-exponential coefficient were calculated using a temperature integral approximation method with Senum and Yang's 4th degree rational approximation [29].

### 2.3. Experimental procedure and test rig

The main experiment investigated the decomposition of toluene, a tar-representing, methylated aromatic compound, during its pyrolytic conversion that was catalysed by wood-derived char. The change in the toluene conversion efficiency with reaction time was investigated by varying the feeding time within the range of 5–60 min. Three series of tests, one for each of the examined chars, were performed. Additional experiments with a modified measurement procedure were also carried out in order to investigate the influence of an intermission in the compound's supply and the impact of selected AAEM metals in char on the toluene conversion efficiency.

The experiment was carried out in a laboratory scale reactor comprising three segments: a tar-gas mixture preparation section; a reaction zone; and a sampling train, which have been outlined in Fig. 1. All of the reactants were introduced into the upper part of the quartz tube reactor (20 mm i.d). The selected gases provided the desired atmosphere for the reaction and served as a carrier for the liquid compounds. If required, the set-up allowed for steam generation by supplying water via a syringe pump (1). A tar-representing compound was fed, by means of the second channel of the pump (2), through a sealed opening in the reactor. The liquid compounds were captured on a quartz wool plug (3) in the upper heating zone (4) set at 200 °C. In this study, only toluene with a constant concentration of 12 g/Nm³ in a pure $N_2$ flow was used in each test. After evaporation and mixing with the permanent gases, all of the reactants entered the 300 mm long reaction zone (5). The reactants travelled through a catalyst bed, i.e. 0.5 g of char (6) placed between quartz wool plugs (7) in the middle of the reaction zone, which was held at 800 °C. The char bed had a height of approximately 15 mm, resulting in a gas residence time of 0.1 s, on the assumption of a 0.5 void fraction [7]. As the reactor-to-particle diameter ratio was >15, a flat velocity profile and no preferential flows could be assumed [30]. Accounting for the temperature profile inside the reactor, the gas

residence time at temperatures greater than 790 °C was approximately 1 s. The products of the conversion reactions were then transferred via a heated line to a sampling train comprising two impinger bottles (8), one kept at ambient temperature and the other in a −25 °C bath, and a gas bag (9). The unreacted fraction of the tar compound and the condensable products of its conversion were collected in the impinger bottles throughout the entire experimental run. Permanent gases were captured in a series of gas bags, which were changed at intervals of 90 s. After the desired toluene feeding time was reached, the toluene feeding line (1) was removed from the reactor and the spent char bed was cooled down to ambient temperature in a $N_2$ flow and stored in a desiccator. The liquid and gaseous products were analysed post-run with an Agilent 6890N chromatograph using flame ionization detector (FID) and thermal conductivity detector (TCD), respectively. The conditions for the analysis of the liquid products have been detailed in the previous work [27]. Gaseous samples were collected during each of the 30 and 60 min runs; in order to analyse these samples, a J&W GS-CarbonPLOT 30 m × 0.53 mm × 3 μm capillary column, followed by J&W HP-PLOT 30 m × 0.53 mm × 25 μm molecular sieves were used. For the duration of the $CO_2$ elution, the molecular sieves were bypassed by means of a 6-way valve, in order to avoid $CO_2$ retention and clogging of the sieves.

High-grade compressed gases were supplied by Air Liquide (He with a purity of 99.9999% and the others with a purity of 99.999%) for the purpose of operating the analytical instruments and the test rig. $H_2$ (99.999%) was generated *in situ* with a SPE150HC hydrogen generator. Anhydrous toluene with a purity ≥ 99.8% was obtained from Sigma Aldrich to represent tar. Dichloromethane with a purity ≥ 99.8% from Sigma Aldrich was used as the solvent for sampling the liquid products. Standard solutions for calibration of the FID were prepared with reagents (purity ≥ 99.0%) from Sigma Aldrich, MERCK and Avantor Performance Materials Poland S.A.

The air-tightness of the reactor and the feeding system, as well as the efficiency of the sampling train, were verified by performing tests with an empty reactor and both furnaces set to 200 °C; under these conditions, when no conversion was expected, toluene recovery was maintained above 98%. Additionally, prior to the main catalytic conversion experiments, a test at a target experiment temperature of 800 °C was performed without a char bed. Although some toluene decomposition has been previously observed under increased pressure or reactive atmospheres [12,31], toluene recovery in five consecutive tests was maintained above 96%. Thus, it was concluded that, under the inert condition of this study, any homogeneous thermal conversion was negligible.

All of the toluene catalytic conversion tests were performed under an inert atmosphere and their parameters have been summarised in Table 1. The main experiment (tests 1–3) allowed for the catalytic performance of three woody biochars to be compared. Tests 4–5 were performed to assess the influence of interrupting the dosing of toluene on its removal efficiency and the distribution of its products. To this end, the continuous and steady feeding rate of the toluene, applied during tests 1–3, was paused after an initial 10 or 15 min, so that $N_2$ was purging the reactor for 15 min. Afterwards, the toluene dosing was resumed and continued until a total feeding time of 30 min was reached. A separate set of impinger bottles was used for each part of the intermittent feeding; this enabled both the partial and overall toluene conversions to be calculated. Other additional tests (6–7) were aimed at assessing the potential of alkali and alkaline earth metals (AAEM) to catalyse the decomposition of hydrocarbons. A 30 min toluene conversion test was repeated with activated alder chars that had been subjected to acid washing and $Na^+$ impregnation; thus, chars with a modified metal content were obtained.

### 2.4. Calculations

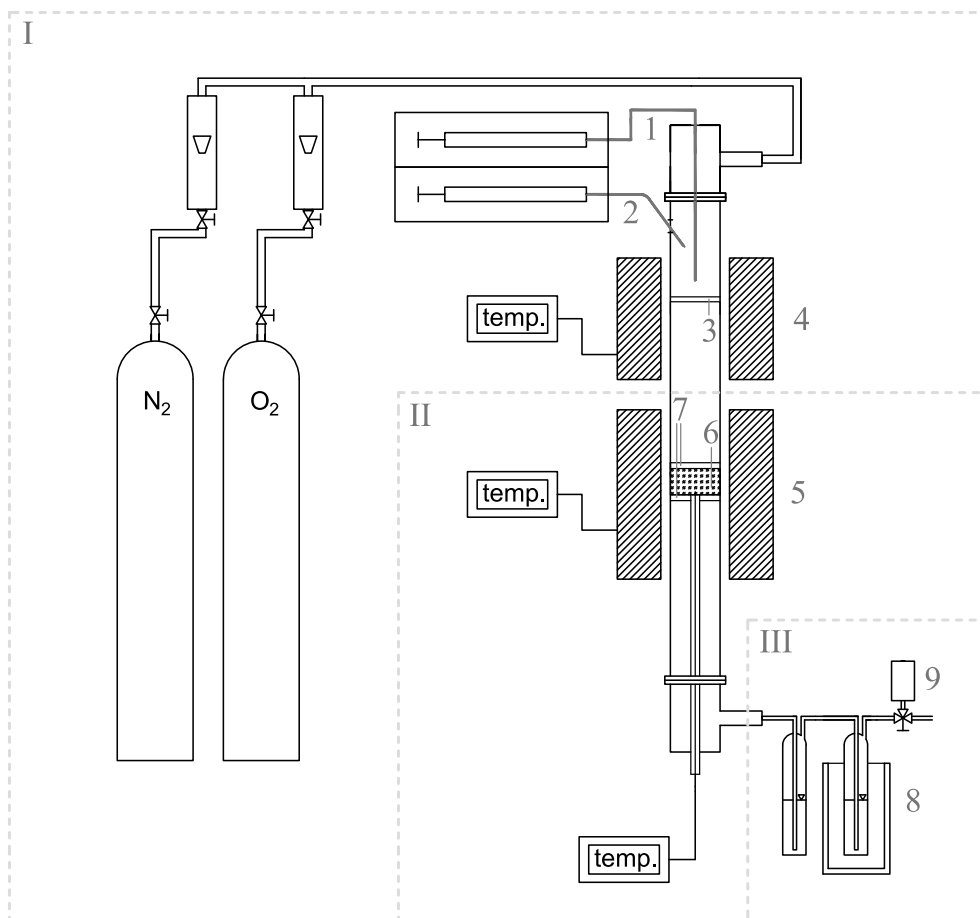Toluene conversion ($\eta_T$) was determined from the equation:

**Fig. 1.** The test rig: I – gas mixture preparation section, II – reaction zone, III – sampling train (1 – capillary for water feeding, 2 – tubing for tar compound feeding, 3 – quartz wool; 4 – evaporator, 5 – reaction zone with catalyst, 6 – char bed, 7 – quartz wool, 8 – impinger bottles, 9 – gas bag).

$$\eta_T = (m_{Tf} - m_{Tr})/m_{Tf} \tag{1}$$

where $m_{Tf}$ is the mass of the toluene fed into the reactor (mg) and $m_{Tr}$ is the mass of toluene recovered at the reactor outlet (mg). The relative molar yields of the liquid by-products ($x_i$) were based on the amount of converted toluene and calculated from the equation:

$$x_i = m_i/(m_{Tf} - m_{Tr}) \cdot M_T/M_i \tag{2}$$

where $m_i$ is the mass of the $i$-th recovered by-product (mg), and $M_T$ and $M_i$ denote toluene's and i-$th$ compound's molar masses (mg/mmol), respectively.

Since the gas sampling interval was 1.5 min and the experimental run times were t = {5,10,20,30,40,50,60} min, the relative molecular yield of the $i$-th gas species for the $t$-time run ($x_{i,t}$) was calculated according to the equation:

$$x_{i,t} = \frac{\sum_{n=1}^{n=n_t} ([i]_n/[N_2]_n \cdot \dot{n}_{N_2} \cdot \tau_{int})}{n_{T,t}} \tag{3}$$

where, $[i]_n$ is the concentration of the $i$-th gaseous species detected in the $n$-th gas bag (vol.%), $[N_2]_n$ is the concentration of $N_2$ in the $n$-th gas bag (vol.%), $\dot{n}_{N_2}$ is the molar flow of $N_2$ fed into the reactor (mol/min), $\tau_{int}$ is the sampling interval (min), and $n_{T,t}$ is the amount of toluene (mol) converted during an experimental run with a feeding time $t$.

Since the construction of the test rig did not allow for gravimetric determination of the coke deposit, its yield ($m_{cc}$) was calculated from a carbon based mass balance as follows:

$$m_{cc} = m_{cTf} - \sum (m_{cTr} + m_{cG} + m_{cB} + m_{cSB}) \tag{4}$$

where, $m_c$ is the mass of the carbon (mg) in $c$ – coke, $Tf$ – fed toluene, $Tr$ – recovered toluene, $G$ – gaseous species, $B$ – benzene, and $SB$ – substituted benzenes.

All of the experiments were duplicated and the average values were

**Table 1**

Summary of the tests of the catalytic conversion of toluene in a $N_2$ flow: main experiment (1–3), intermittent feeding tests (4–5), and the AAEM tests (6–7).

| No. | Char feedstock | Feeding time, min | Feeding mode | Char modification |
|---|---|---|---|---|
| 1 | Alder | 5, 10, 20, 30, 40, 50, 60 | Continuous | None |
| 2 | Beech | 5, 10, 20, 30, 40, 50, 60 | Continuous | None |
| 3 | Pine | 5, 10, 20, 30, 40, 50, 60 | Continuous | None |
| 4 | Alder | 30 | Intermittent 10 + 20 min | None |
| 5 | Alder | 30 | Intermittent 15 + 15 min | None |
| 6 | Alder | 30 | Continuous | HCl washing |
| 7 | Alder | 30 | Continuous | HCl washing Na$^+$ impregnation |

**Table 2**

The composition of the wood samples used for preparation of the biochar; VM – volatile matter, ASH – ash, FC – fixed carbon.

| Elemental composition, wt.% daf (standard deviations of two replicates) | | | | |
|---|---|---|---|---|
| | C | H | N | S | O (by diff.) |
| Alder | 50.28 ± 1.42 | 6.26 ± 0.27 | 0.32 ± 0.30 | 0.02 ± 0.01 | 43.12 |
| Beech | 49.77 ± 1.34 | 6.14 ± 0.25 | 0.22 ± 0.01 | 0.01 ± 0.01 | 43.86 |
| Pine | 52.57 ± 1.48 | 6.29 ± 0.28 | 0.12 ± 0.01 | 0.01 ± 0.01 | 41.01 |

| Proximate analysis, wt.% dry (standard deviations of two replicates) | | |
|---|---|---|
| | VM | ASH | FC (by diff.) |
| Alder | 84.7 ± 3.9 | 0.44 ± 0.02 | 14.86 |
| Beech | 84.4 ± 3.9 | 0.51 ± 0.02 | 15.09 |
| Pine | 87.4 ± 0.5 | 0.20 ± 0.01 | 12.41 |

| Chemical composition, wt.% dry (standard deviations of three replicates) | | | |
|---|---|---|---|
| | cellulose | hemicellulose | lignin | extractives |
| Alder | 42.46 ± 0.06 | 33.67 ± 2.17 | 23.71 ± 0.45 | 3.68 ± 0.34 |
| Beech | 39.53 ± 0.20 | 37.11 ± 0.65 | 20.97 ± 0.46 | 2.54 ± 0.13 |
| Pine | 44.10 ± 0.25 | 27.81 ± 1.52 | 29.75 ± 0.20 | 7.14 ± 0.08 |

taken and reported. The pooled standard deviations were plotted, along with the toluene conversion and the yields of the products. An analysis of variance (ANOVA) was used to assess the significance of the differences between the obtained datasets, as has been shown to be suitable in similar experiments [6,32]. A comparison of the toluene conversion was performed between the measurement series carried out with alder and pine, alder and beech, and pine and beech chars.

## 3. Results and discussion

### 3.1. Raw wood characteristics

The decomposition of the tar compounds was catalysed with biochars prepared from three tree species in order to provide an overview of the different wood types: a coniferous softwood (pine); a relatively softdeciduous hardwood (alder); and a typical deciduous hardwood (beech). The composition of the selected feedstocks and their FTIR spectra have been presented in Table 2 and Fig. 2, respectively. All of the materials had a similar elemental and proximate composition, and while the distribution of their chemical components was typical for

each species, it differed among the samples. Pine, as a coniferous tree, had significantly more extractives, due to a presence of resin acids (represented by the 1697 cm$^{-1}$ band in the FTIR spectrum), and contained more lignin, compared to the two deciduous trees. Moreover, the structure of pine lignin differed from that of the lignin of the deciduous trees, as confirmed by the FTIR analysis. Coniferous wood lignin is comprised mostly of guaiacyl units; their presence was confirmed by a pronounced band at 1265 cm$^{-1}$, which originated from the ring breathing, and at 808 cm$^{-1}$, from the C–H vibration. Moreover, the relative intensities of the bands $1265 \gg 1236$ cm$^{-1}$ and $1505 \gg 1594$ cm$^{-1}$, respectively, suggested a higher lignin/holocellulose ratio and the predominance of G-type lignin in the pinewood. The coexistence of guaiacyl and syringyl units in the lignin of the deciduous trees was confirmed by the increased absorption at 1265 cm$^{-1}$ as well as 1327 cm$^{-1}$ in the alder and beech spectra [33–35].

Beech had a low lignin content, which is typical for hardwoods; as a softer material, alder had a chemical composition that was slightly closer to that of pinewood. However, their matching FTIR spectra suggested that, despite a quantitative difference in the content of their polymeric constituents, their structure was similar for both deciduous woods. All of the above observations are in alignment with the characteristic differences between coniferous and deciduous trees, as well as softwoods and hardwoods [36].

### 3.2. Characterization of the active sites of the char

The toluene conversion was possible due to the catalytic properties of the wood-derived activated chars. No removal was detected during the blank tests, where the toluene was fed into an empty reactor, indicating the lack of homogeneous, thermal decomposition under the applied conditions. Additionally, a batch of non-activated char was examined – the preparation process was terminated after the first stage, i.e. pyrolysis for 60 min at 800 °C in pure $N_2$. It was reported in the literature that some chars that were prepared under milder conditions or reactive atmospheres were able to catalyse the tar decomposition without any additional treatment [6,9]. However, due to the relatively high temperature and the long time of the pyrolysis during the char preparation in this study, the non-activated material had poor catalytic properties, as detailed in the previous work [27]. A 10 min toluene conversion over non-activated pine char was carried out according to the procedure that was applied during the main experiments. This test revealed that, prior to activation, the properties of the char were not
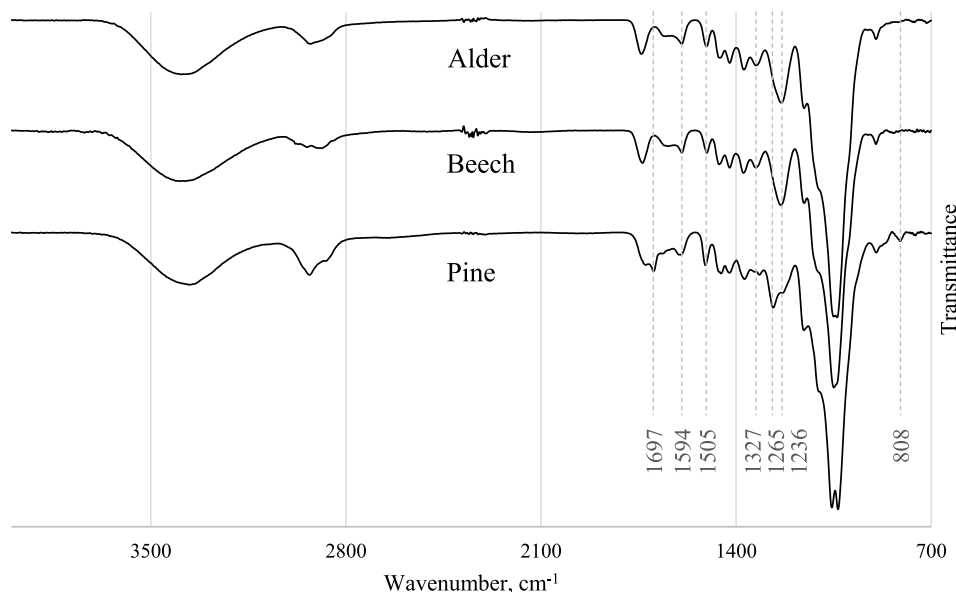


**Fig. 2.** ATR-FTIR spectra of the pulverised samples of the wood used for preparation of the biochar.
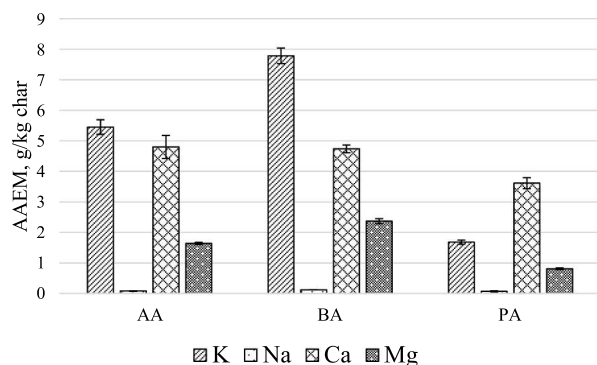
**Fig. 3.** AAEM species content in activated chars from alder (AA), beech (BA) and pine (PA).

sufficient to initiate any toluene removal. Thus, it has been established that the presence of a catalytically inclined material is crucial for toluene decomposition under the examined conditions, and that the chars gained the required catalytic properties upon the activation step of their synthesis.

The main features attributed to the catalytic behaviour of carbonaceous materials are the active surface sites, usually identified as AAEM species and O-containing functional groups, as well as defects in the carbon lattice, generally termed as "unsaturated carbons". Moreover, the surface area and pore distribution in a char particle is believed to be of high importance as they provide support and thus determine the availability of all of the abovementioned surface structures. Therefore, some physicochemical properties of the prepared chars were examined in order to allow for correlation of their structure with their catalytic performance during the toluene pyrolytic conversion.

### 3.2.1. Alkali and alkaline earth metals

The content of the four main alkali and alkaline earth metals (AAEM) in all of the three chars was analysed, as shown in Fig. 3. These elements have a well-documented catalytic effect on the kinetics of the oxidation of carbonaceous materials [22]. The highest impact on the gasification reactivity of char has been commonly assigned to K, followed by Na, Ca and Mg [21]. The most important of the quantified inorganic species, potassium, was also the most abundant element in chars from deciduous-trees, especially in beech char. Pine char comprised significantly less K; Ca was identified as the main AAEM in this sample. All of the studied chars comprised negligible amounts of Na; Mg concentrations were relatively low as well. Ca concentration was moderate and similar in all of the examined chars. A generally higher AAEM concentration in the chars of the two deciduous-trees was expected to enhance their reactivity during oxidation reactions, compared to the pine char.

### 3.2.2. Surface functional groups

Although most substituents with heteroatoms are released from biomass upon its devolatilisation, thermal activation of carbonaceous materials can create some O-containing surface groups. These structures, with either acidic or basic character, are expected to act as active sites during catalytic conversion of hydrocarbons. A simple assessment of the functionalities of the char was made based on the ATR-FTIR spectra of their surfaces, which have been presented in Fig. 4. Common features of the examined samples were the main absorption regions at $1630 - 1420 \, cm^{-1}$ and $1300 - 900 \, cm^{-1}$. No increased absorption was registered at higher wavenumbers; this suggests that there were no significant amounts of –OH or aliphatic groups on the surfaces of the chars. Thus, the spectra in Fig. 4 were trimmed to show only wavenumbers below $2200 \, cm^{-1}$ to increase the readability of the most important area. The absorption at $1630 - 1420 \, cm^{-1}$ can be attributed to

two types of structures. One of them comprises aromatic rings; their presence is additionally confirmed by the ring stretching overtones at $2000 - 1660 \, cm^{-1}$ and increased absorption at the C–H bending region, at $900 - 700 \, cm^{-1}$. Another plausible structure, which overlapped the absorption frequencies of the fundamental and overtone frequencies of the stretching aromatic rings, is the C=O bond that is present in numerous surface functionalities. The most pronounced absorption can be observed within the fingerprint region, i.e. $1300 - 900 \, cm^{-1}$; miscellaneous single bonds, e.g. C–O and C–C, absorb at these frequencies [37,38]. The intensity of the absorption in the two main regions represents general magnitude of the development of the O-containing functional groups, e.g. free carboxylic acids, acid esters, lactones, ketones and quinones.

The obtained spectra did not unambiguously determine what structures were present on the surface of the char. However, they indicated a range of possible conformations that were in alignment with the functionalities that have been previously reported in studies on carbonaceous materials [16,39,40]. The carbonyl groups, C–O–C conformations, and aromatic rings were the structures that were most likely to be found in the examined chars. No significant amount of aliphatic or hydroxyl substituents were found on the surfaces of the char, thus, it is expected that phenolic and carboxylic groups were present in the form of ethers and esters, rather than in a free, protonated state.

A comparison of the spectra of the chars suggested that all the samples had some aromatic structures, along with oxygen functionalities, mainly in the form of carbonyls and oxygen bridges. However, higher intensity within the $1200 - 1000 \, cm^{-1}$ region suggested that the alder and beech char surfaces contained more groups with an acidic character, such as carboxylic acid anhydrides. Pine char, on the other hand, plausibly had an increased amount of aromatic rings and basic sites such as carbonyls, as indicated by the more pronounced $1900 - 1700 \, cm^{-1}$ and $1500 - 1350 \, cm^{-1}$ bands. The transformation from raw wood to activated char occurred with an intermediate step of pyrolysis under a reducing atmosphere when most of the functional groups of char were decomposed, before being re-created upon interaction with steam. However, it should be noted that pinewood, which was more abundant in aromatic rings due to its higher lignin content, produced activated char that was plausibly more aromatic. Alder and beech chars, on the other hand, had more C–O structures, as their precursors had a higher hemicellulose content.

The functionalities of acidic nature present on the surface of chars were quantified using the Boehm titration method. The distributions that were obtained for the three types of acidic sites, with gradually increasing strength, have been presented in Table 3. On all of the surfaces of the examined chars, the strongest acidic sites, i.e. carboxylic acids, were the most abundant. Significantly smaller amounts of weaker groups (lactonic and phenolic) were also detected. The ANOVA analysis of the obtained results suggested that there were no significant differences between the alder (AA) and beech (BA) chars. However, the distinction between the chars from the coniferous and deciduous trees was found to be statistically significant. This observation correlates well with the similarity of the AA and BA char FTIR spectra and their discrepancy from that of pine char (PA). The distribution of the acidic sites suggested that the main difference lay in the amount of carboxylic groups. Thus, it can be expected that the $1200 - 1000 \, cm^{-1}$ region of the char spectra, which was more pronounced for AA and BA, originated from esters and anhydrides; these, upon titration pre-treatment, underwent protonation to carboxylic functionalities that were detected with the Boehm method.

The oxygenated functionalities were also assessed using a temperature programmed desorption (TPD) experiment performed via the TGA-FTIR technique. Activated alder char was heated to 1000 °C under a nitrogen flow in a thermogravimetric analyser. Measurement of the sample's mass loss was coupled with an online collection of the spectra of the gases released from the char during the treatment. Unfortunately,
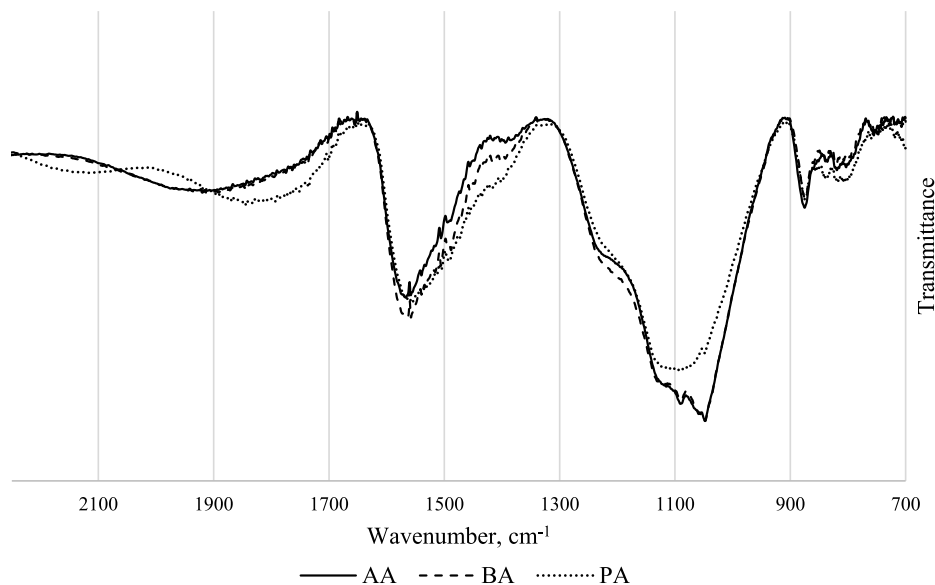
**Fig. 4.** ATR-FTIR spectra of activated chars from alder (AA), beech (BA) and pine (PA).

**Table 3**
Acidic sites distribution (with increasing strength) on the surface of the activated alder (AA), beech (BA) and pine (PA) chars, determined by the Boehm titration method.

| Acidic sites type, μeq/g | AA | BA | PA |
|---|---|---|---|
| phenolic | $72 \pm 08$ | $71 \pm 13$ | $69 \pm 06$ |
| lactonic | $50 \pm 08$ | $43 \pm 03$ | $57 \pm 14$ |
| carboxylic | $201 \pm 04$ | $208 \pm 02$ | $149 \pm 14$ |

the poor response of the FTIR instrument, despite the large mass of the sample, provided only qualitative insight into the types of the decomposed functional groups. The evolution profiles of CO and $CO_2$ have been plotted in Fig. 5, along with the first derivative (DTG) of the char's mass loss curve. Four main decomposition steps could be distinguished and were assigned to the characteristic surface structures of carbonaceous materials [16,40–42]. The first DTG peak, at 365 °C, was correlated with the release of a small amount of $CO_2$. Lower temperatures are commonly attributed to the decomposition of acidic sites, thus the initial loss of mass might result from the thermal destruction of carboxylic
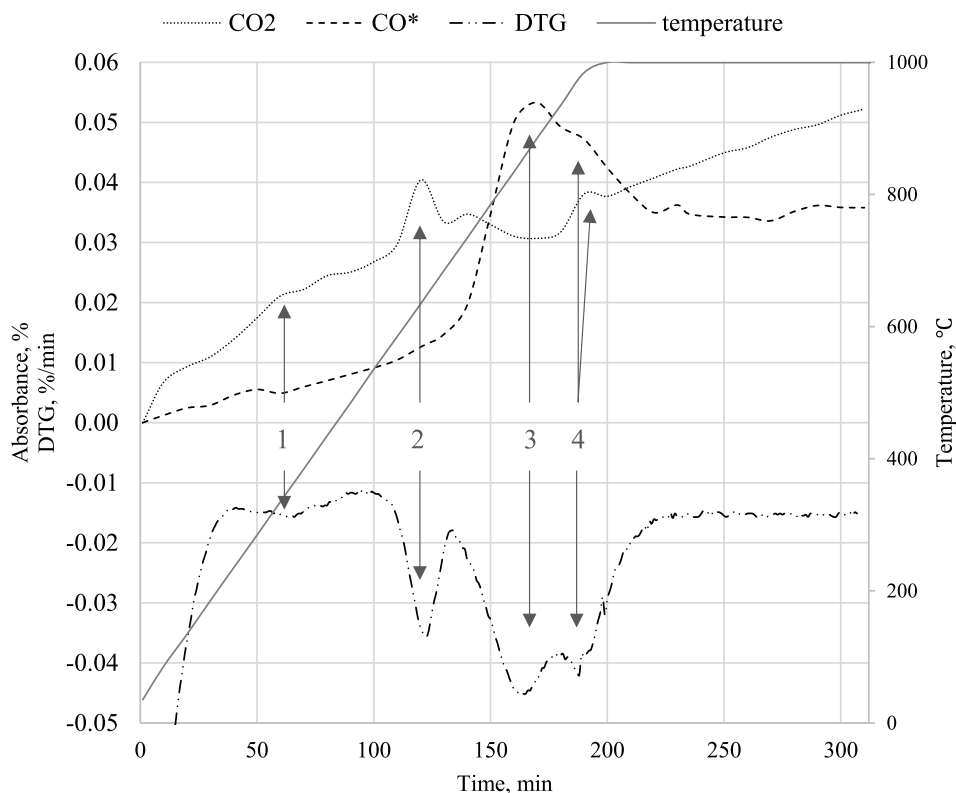


**Fig. 5.** Temperature programmed desorption of activated alder char using the TGA-FTIR method: released $CO_2$ and CO (* x10 magnified) IR absorbance, DTG of char mass loss, and temperature profile (1–4 – characteristic peaks from the decomposition of specific functional groups).

acids. The second peak, at 635 °C, originated from acidic structures, such as acid anhydrides and lactones, which also yielded $CO_2$. At higher temperatures, the formation of CO prevailed. A third mass loss region, at 860 °C, released CO, some of it possibly originating from the destruction of phenolic groups, although, at these temperatures, basic structures such as carbonyls and quinones also begin intense decomposition. CO and small amounts of $CO_2$ that were created above 900 °C (fourth peak) corresponded with the breakdown of basic pyrone and chromene-like structures in the carbon matrix [40,43–45]. The intense desorption from the surface of the char at high temperatures suggested an abundance of basic functional groups, which were not quantified with the Boehm method. These structures are often observed in materials that are activated by thermal methods, as opposed to acidic sites that are created in abundance during chemical activation [16].

All of the examined chars acquired some functional groups due to steam activation; they were present in the form of O-containing structures of both acidic and basic nature. The TGA-FTIR analysis suggested that the basic functionalities were more abundant, as expected during thermal activation. The ATR-FTIR and Boehm titration analysis revealed some differences between the coniferous pine and the deciduous alder and beech chars. Pine char generally had fewer functionalities of an acidic nature, especially strong carboxylic ones. However, it had more pronounced aromatic and/or basic sites. Due to the consistent method that was used to prepare all of the examined chars, the observed differences were thought to originate from the inherent properties of the different wood types, e.g. the lignin structure and content. The functional groups that are present in the raw wood decompose during pyrolysis, yet their release is expected to leave some defects in the carbon structure that can constitute active sites that are prone to thermal activation [16]. Therefore, it can be concluded that the properties of the raw wood are correlated with the extent of the re-creation of the O-containing, acidic structures during the steam activation step of char preparation.

### 3.2.3. Surface area and porosity

All of the potential active sites, i.e. the functional groups, the AAEM species and the "unsaturated carbons" are distributed on the surface of the catalyst. Although heterogeneous conversion over a carbonaceous material is expected to occur exclusively with those structures, the overall char morphology, i.e. its surface area and pore distribution, determines the accessibility and dispersion of the active sites [41]. Thus, the physical properties of the char are particularly important. The well-developed structure of the carbonaceous matrix provides good support for the catalytically active surface sites, while pore size and shape affects the diffusional mass transfer of the reactant towards these sites. Therefore, the BET surface area calculation and an estimation of the micropore area were conducted to further assess the catalytic affinities of the studied samples.

The structural features of the chars, based on the nitrogen adsorption measurements, have been presented in Fig. 6. All of the chars had a highly developed total surface area with significant contribution from the micropores; both deciduous tree chars had almost exactly the same structure. The total surface area of the pine char was 40 $m^2$/g smaller than the other samples, yet it had smaller pores. The share of the micropores in the pine char reached 75%, while it was only 59% and 60% for the alder and beech chars, respectively. This discrepancy between the chars of the coniferous and deciduous trees was expected to play a major role in their different catalytic performance, as described further in Section 3.3.

### 3.2.4. TGA oxidation kinetics

Char, as a carbon-based material, undergoes oxidation reactions with gasifying agents such as steam, $CO_2$ or $O_2$; the thermal activation process also involves these reactions. Thus, the reactivity of a char can influence the extent of the morphological changes evoked by the activation process and consequently determine its suitability as a catalyst
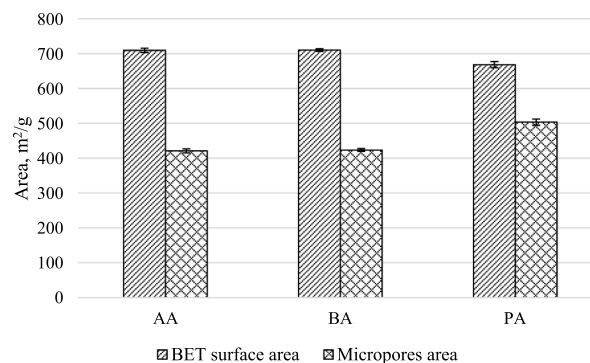


**Fig. 6.** The BET surface area and the micropores area of the activated chars from alder (AA), beech (BA) and pine (PA).

**Table 4**
Kinetic parameters for activated alder (AA), beech (BA) and pine (PA) char TGA oxidation and the temperature range of the region considered for a 3 – 10% mass loss.

|  | AA | BA | PA |
|---|---|---|---|
| Activation energy ($E_a$), kJ/mol | 74 | 50 | 143 |
| Pre-exponential coefficient ($A$), 1/s | $7.0 \cdot 10^1$ | 1.6 | $6.7 \cdot 10^6$ |
| Coefficient of determination ($R^2$), – | 0.9901 | 0.9981 | 0.9949 |
| Temperature range, °C | 390 – 542 | 346 – 420 | 433 – 470 |

precursor. Thermogravimetric analysis of the oxidation of the chars with $O_2$ was then conducted to calculate its kinetic parameters (Table 4) and thus provide feedback on the reactivity of the studied materials. The results showed that the activation energy of the pine char was substantially higher and that the reaction was initiated at higher temperatures, compared to the chars from the deciduous trees. It should be noted that significant discrepancies were also registered between the alder and beech chars, despite their relatively similar physicochemical properties. The only other difference that was observed between these chars was an increased amount of potassium and magnesium in the beech char. As the catalytic effect of the AAEM species on carbon oxidation is a well-recognised phenomenon [21,22], their diversified content was, most likely, responsible for the observed spread in the reactivity of the chars. It is therefore plausible that pine char, due to a lower metal content, was less susceptible to steam activation, which is often correlated with pore widening [20,46]. This could explain the less developed mesoporosity of this material.

### 3.3. Toluene pyrolytic conversion

The toluene conversion ($\eta_T$) during its catalytic pyrolysis, calculated from Eq. (1), has been presented in Fig. 7. The continuous decrease of $\eta_T$ with time, which was noticeable for all of the catalysts that were studied, can be attributed to coke deposition on the surface of the chars. This phenomenon of the formation of a dense, carbon-rich layer is known to deactivate catalysts by blocking their pores and occupying their active sites [2,5]. The main difference in the performance of the three studied materials occurred between the pine char (PA) and the chars from the deciduous trees – from alder (AA) and beech (BA). Firstly, the toluene conversion was significantly lower throughout the whole process and secondly, the deterioration in its efficiency progressed more rapidly when PA was used. The former observation is evidence of the worse catalytic properties of PA, while the latter suggests quicker deactivation of the pine char due to coke deposition. The close resemblance between the $\eta_T$ plots for the BA and AA char suggests those samples possess similar catalytic properties for hydrocarbon conversion.

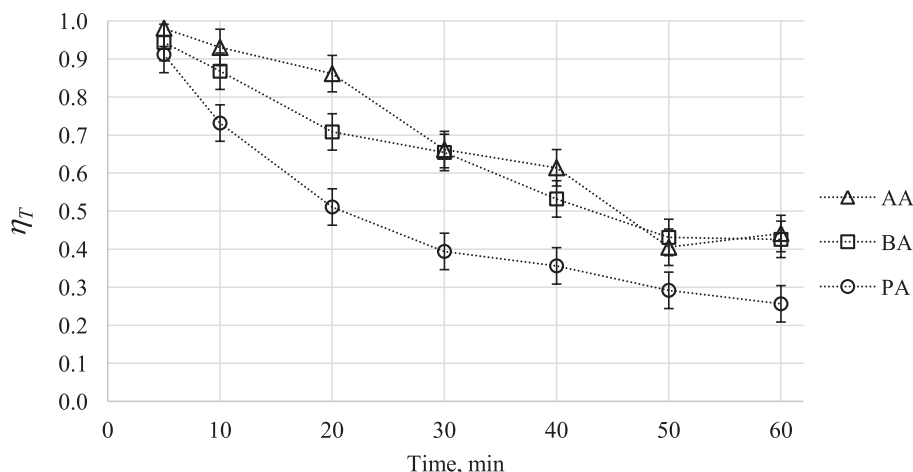The steam activated chars acquired some O-containing functional

**Fig. 7.** Toluene conversion against time during pyrolysis over alder (AA), beech (BA) and pine (PA) chars.

groups. Although basic sites were more abundant, the increased content of the strongly acidic sites in the deciduous trees chars likely contributed to the enhanced catalytic performance of those materials. Their formation was most likely dependent on the chemistry of the raw wood, as it is most likely that they were created on sites of defects in the carbon structure that were created during feedstock decomposition. Therefore, it can be expected that, despite their poor thermal stability, the functionalities of the wood can contribute, along with the conditions for char formation, to the performance of the produced catalysts. Another important structural feature of the chars is their mesoporosity. The findings suggest that the lower content of AAEM species in the pine char resulted in the lower oxidation reactivity of this material, thus the mesopore-favouring effect of the steam activation was less pronounced, which created a more microporous catalyst with impaired longevity. Therefore, it can be expected that the inorganic and chemical constituents of the wood can influence the properties of the obtained chars, therefore indirectly influencing their catalytic performance.

Benzene was the main liquid by-product of the toluene decomposition. Although the overall amount of benzene that was created was lower during the experiments with pine char, when accounting for the lower toluene conversion over this catalyst (Eq. (2)), the relative yields that were obtained for all three materials were statistically similar, as shown in Fig. 8. For each experimental series, an increase in the benzene yield can be seen during the initial 20 min of toluene feeding.

Prolonging this process resulted in a steady toluene-to-benzene conversion with a selectivity of ~12 – 16%. Apart from benzene, small amounts of substituted, single-ring compounds were also created. The three peaks that were detected during the GC-FID analysis of contents of the impingers were identified as: ethylbenzene; *p*-xylene/*m*-xylene; and *o*-xylene/styrene. Due to the peaks overlapping, two possible compounds could be ascribed to the last two peaks; average molecular weights were then incorporated into Eq. (2) in order to calculate the relevant yield of the substituted benzenes, as shown in Fig. 9. The relative yields have been presented in order to show the toluene selectivity towards the formation of by-products, yet the total amount of substituted benzenes also increased with time of the experiments. The formation of these compounds was enhanced during prolonged experimental runs, and again, it was not affected by the type of char that was applied – apart from a slightly higher ethylbenzene yield during tests with the pine char. An analysis of the released gases revealed that some $H_2$ and $CH_4$ was formed during the heterogeneous conversion of toluene (Fig. 10). No CO or $CO_2$ was detected in the analysis, suggesting that neither char devolatilisation nor toluene decomposition through ring opening occurred during the experiments. The yields of the released gases were similar for all of the chars that were studied, the only difference being that the evolution profiles for the pine char runs peaked at shorter times; this was most likely due to the more rapid deactivation and shorter longevity of this catalyst.
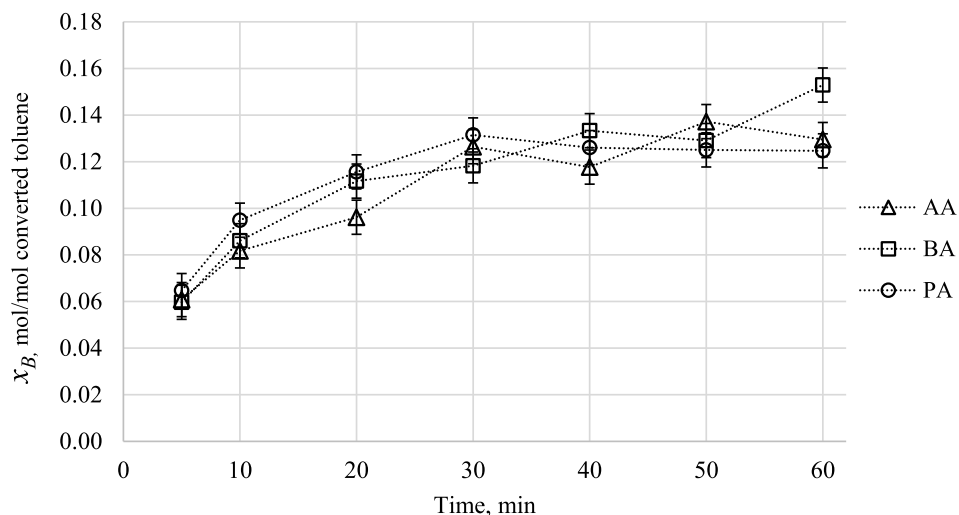


**Fig. 8.** Relative benzene molecular yield (converted toluene based) from pyrolytic toluene conversion over alder (AA), beech (BA) and pine (PA) chars.
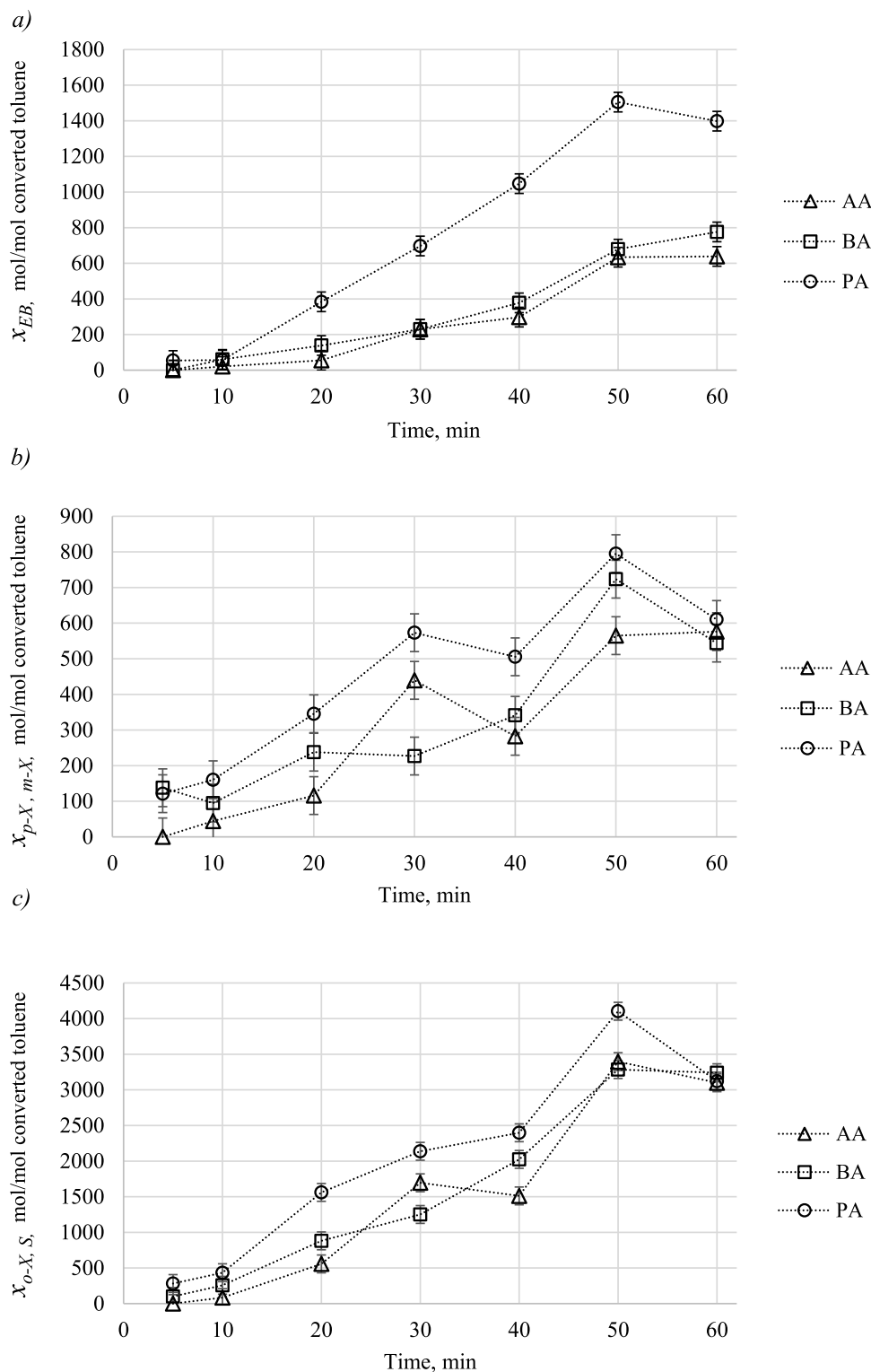
**Fig. 9.** Relative molecular yields of substituted benzenes (converted toluene based) a) ethylbenzene, b) *p*-xylene and/or *m*-xylene, c) *o*-xylene and/or styrene created during toluene pyrolytic conversion over alder (AA), beech (BA) and pine (PA) chars.

The yield of the coke that was created on the char bed was calculated from a C mass balance (Eq. (4)). As shown in Fig. 11, the intense coke formation occurred at the initial stages of catalytic decomposition of the toluene. The gradual saturation of the char with deposited carbon inhibited further growth of the coke layer, thus decreasing the toluene conversion. Pine char, due to its higher microporosity, had a lower capacity for coke, thus a lower deposit yield was observed for this material.

The main role of the char bed during pyrolytic conversion of toluene was to provide an active surface for the heterogeneous reactions of both coking and demethylation; no direct toluene decomposition pathways were observed in this study, e.g. non-catalytic or thermal cracking. However, as a product of the biomass devolatilisation and steam gasification, the char bed could become thermally unstable, resulting in the
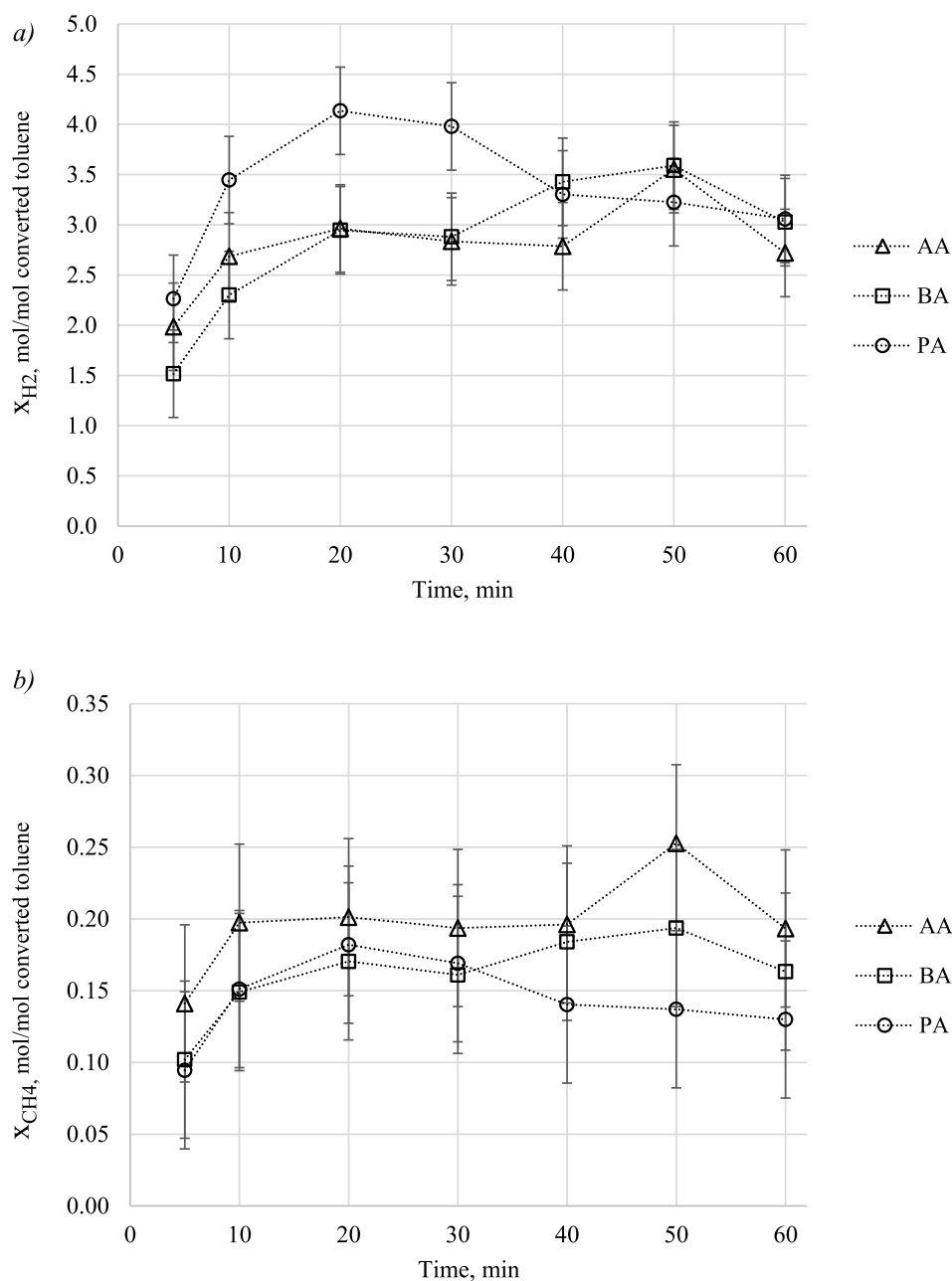
Fig. 10. Relative molecular yield (converted toluene based) of $H_2$ and $CH_4$ released during toluene pyrolytic conversion over alder (AA), beech (BA) and pine (PA) chars.

release of some reactive volatile compounds inside the heated reaction zone. Therefore, another possible pathway of toluene decomposition could be homogenous chain reactions with the free radicals released from the char. This scenario was investigated by conducting an intermittent feeding test. To this end, the dosing of the toluene into the reactor was paused during the test in order to remove any volatile compounds, which might be released from the char surface, from the reaction zone. This treatment should cause any potential chain reactions of the homogenous decomposition of toluene initiated by the char-derived radicals to cease. Hence, the decreased toluene conversion during the intermittent feeding test, as compared to the continuous feeding tests with the same total dose of toluene, would suggest the occurrence of gas-phase chain reactions induced by the presence of the char bed.

Two intermittent 30 min toluene pyrolysis tests with activated alder char were performed. They have been referred to as "10 + 20" and

"15 + 15", and in each of them the compound feeding was paused after the initial 10 or 15 min of the run, respectively. After purging the char bed with pure $N_2$ for 15 min, the toluene supply was resumed until a total feeding time of 30 min was reached. Separate sampling trains were used for the first and the second part of each run, thus enabling the determination of the partial conversions within each of the intervals, along with the total conversion for the overall run time. A comparison of the intermittent feeding tests with the conventional continuous feeding run has been presented in the first part of Table 5 and in Fig. 12. The results showed that there was no statistically significant difference in the overall toluene conversion for each of the investigated feeding schemes. Moreover, the similar benzene yields suggested that both main conversion pathways were not affected by the interruption in the toluene supply. This observation has confirmed the primary role of the char surface and the heterogeneous nature of the catalytic decomposition mechanisms. However, the yields of some of the secondary
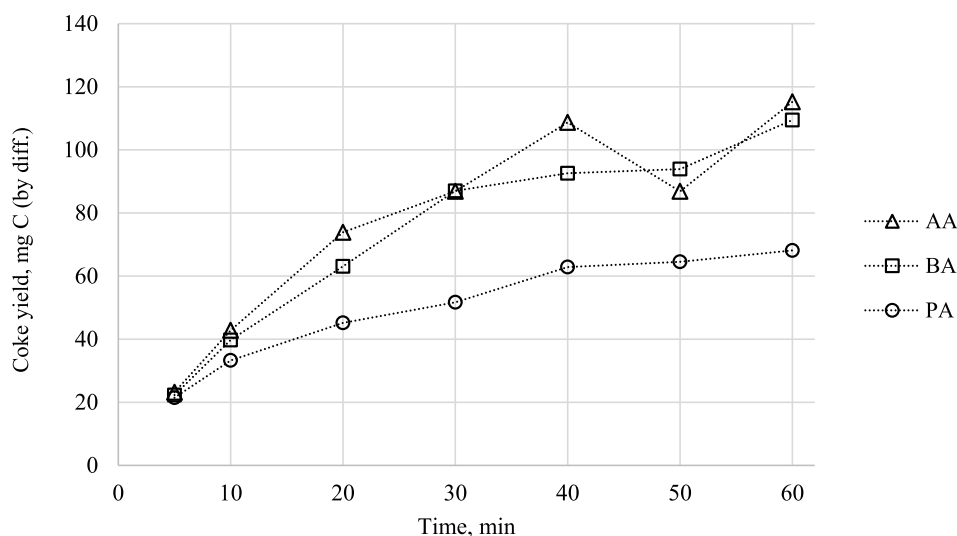
**Fig. 11.** The amount of deposited coke determined from the mass balance for pyrolytic decomposition of toluene over alder (AA), beech (BA) and pine (PA) char.

**Table 5**

Total and partial toluene conversion $\eta_T$ and benzene molecular yield $x_B$ (converted toluene based) for continuous and intermittent feeding during the 30 min pyrolytic conversion tests.

| Total conversion and yield | | | |
|---|---|---|---|
| | 30 min | 15+15 min | 10+20 min |
| $\eta_T$ (±0.05) | 0.66 | 0.64 | 0.69 |
| $x_B$ (±0.01) | 0.13 | 0.11 | 0.11 |

| Partial conversions and yields | | | |
|---|---|---|---|
| | 30 min | | 10+20 min | |
| | first 10 min | second 20 min | first 10 min | second 20 min |
| $\eta_T$ (±0.05) | 0.93 | 0.53 | 0.93 | 0.57 |
| $x_B$ (±0.01) | 0.03 | 0.11 | 0.02 | 0.09 |

continuous 10 min run from the results of the continuous 30 min run allowed for the partial toluene conversion and the benzene yield during the last 20 min of the intermittent and continuous pyrolysis to be compared (Table 5). The results were statistically similar which suggests that the char surface was not affected by the additional 15 min of nitrogen purging at the reaction temperature (800 °C), indicating the thermal stability of this material. Hence, the char deactivation could be attributed solely to the deposition of a coke layer, as no significant thermal annealing was observed.

The information that was obtained about toluene conversion and its by-products allowed the main principles of the pyrolytic decomposition of this compound to be formulated. Deactivation of the char by coke deposition and a simultaneous increase in the yield of the liquid by-products were observed with the prolonged toluene feeding time. Therefore, the toluene conversion at the initial stages of the process most plausibly occurred mainly through coke deposition. Although it remained the paramount conversion pathway throughout the entire experiment, with progressing coke saturation of the char the de-methylation and recombination reactions became more significant, which led to the enhanced formation of benzene and substituted benzenes. The findings also suggest that the conversion via coking was not only preferential but also more efficient, as proven by the decrease in the overall toluene conversion ($\eta_T$) with time, and thus with the
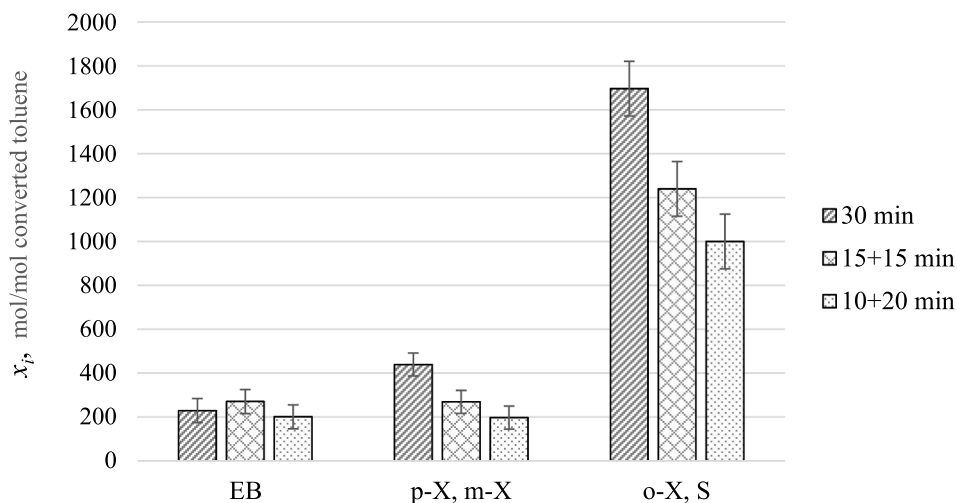
reaction products, i.e. xylenes and styrene, were reduced as a result of the added intermission. The secondary formation of these derivatives involves the gases released from char surface reactions; thus the temporary removal of the heterogeneous conversion products, by purging the bed with nitrogen, inhibited the gas-phase recombination and the creation of substituted benzenes. Partial results of the initial 10 min of the 10 + 20 test were compared with the conventional 10 min run. Subtracting the amount of products that were obtained in the



**Fig. 12.** The relative molecular yields of the secondary reactions products $x_i$ (converted toluene based) for continuous and intermittent feeding during the 30 min pyrolytic conversion runs, where index $i$ represents: EB – ethylbenzene; *p*-X, *m*-X, *o*-X – *p*-, m-, *o*-xylene, respectively; and S – styrene.
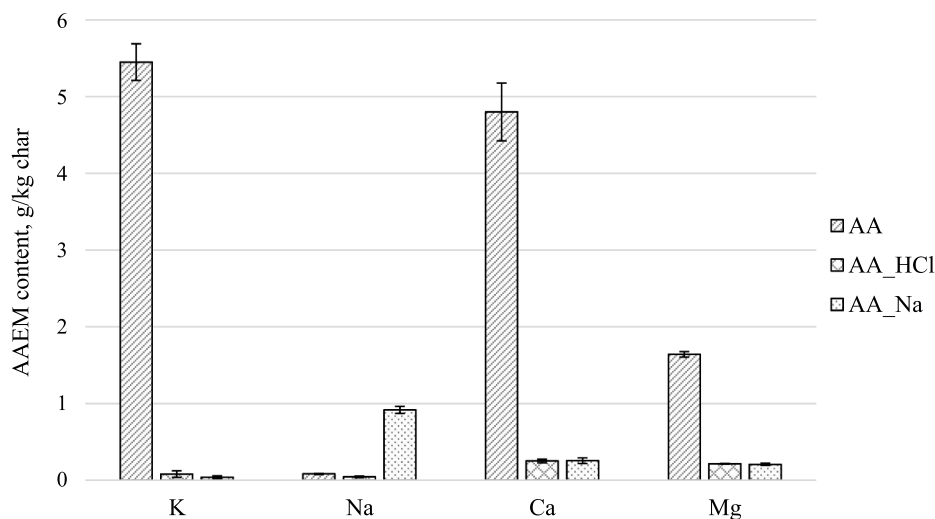
**Fig. 13.** AAEM species content in unmodified activated alder char (AA); in AA char after an HCl wash (AA_HCl); in AA_HCl char after impregnation with $Na^+$ (AA_Na).

**Table 6**

Toluene conversion $\eta_T$ and benzene molecular yield $x_B$ (converted toluene based) during 30 min pyrolytic conversion tests, as well as activation energy $E_a$, pre-exponential factor A and coefficient of determination $R^2$ for TGA oxidation of activated alder char (AA), AA char after an HCl wash (AA_HCl) and AA_HCl char after $Na^+$ impregnation (AA_Na).

| Treatment | AA none | AA_HCl HCl washed | AA_Na HCl washed, $Na^+$ spiked |
|---|---|---|---|
| $\eta_T(\pm0.05)$ | 0.66 | 0.65 | 0.67 |
| $x_B(\pm0.01)$ | 0.13 | 0.11 | 0.11 |
| $E_a$, kJ/mol | 74 | 195 | 135 |
| A, 1/s | $7.0\cdot10^1$ | $2.7\cdot10^9$ | $4.7\cdot10^5$ |
| $R^2$ | 0.9901 | 0.9994 | 0.9993 |

changing ratio between the conversion pathways. Similar behaviour has already been found in the authors' previous studies on pyrolytic conversion of toluene over an activated carbon bed [11]. Since no gas-phase toluene conversion was detected during the preliminary tests with an empty reactor, it is expected that both decomposition pathways, into coke and benzene, occurred heterogeneously, over a char bed. While the distribution of those products altered with the reaction time, a decrease in the overall yields of both compounds was observed. This supports the conclusion about the crucial role of the catalyst's surface during toluene coking as well as demethylation; the latter being most likely responsible for the formation of methane. The relatively similar yields of benzene and $CH_4$ suggested that both compounds originated from the same reaction. This observation is in alignment with the 1-methylnaphthalene decomposition experiments reported by Leininger et al. [47]. In this process, $H_2$ is released due to the dehydrogenation associated with the carbonization of the aromatic rings on the char surface. The gaseous species, released upon the decomposition of toluene into coke and benzene, were likely to be participating in secondary reactions with the continuously fed, fresh compound, leading to the formation of substituted benzenes. Both the relative and overall yields of these secondary products increased with time, indicating that they were less susceptible to the deactivation of the char surface. Among the secondary products, the third group of compounds, comprised of *o*-xylene and styrene, was the most abundant, accounting for up to 3500 ppm of the reacted toluene. It can be expected that the yield of *o*-xylene was not greater than that of the other two isomers, which added up to only 600 – 800 ppm. Thus, styrene was most likely the major substituted benzene that was created during the experiments. The formation of styrene as a part of the third group of the detected

secondary products was confirmed by further analogous tests where tar was represented by *p*-xylene, where its decomposition yielded surprisingly high amounts of *p*-methylstyrene. The most plausible mechanism of the observed secondary reactions was the addition of a methyl group; either directly to the toluene's aromatic ring or to its existing methyl group, creating xylenes or ethylbenzene, respectively. The consecutive, intense dehydrogenation of the ethylbenzene resulted in the abundant formation of styrene.

### 3.4. The effect of the AAEM species

The TGA analysis revealed that there were some differences in the oxidation reactivity of the three wood chars, most likely arising from their various AAEM species content. However, the toluene conversion over the alder and beech char was statistically similar and the only catalyst that showed a handicapped performance was the pine char. Thus, the catalytic performance of the examined samples was related to their microporosity and acidic sites rather than their different content of AAEM species. As the role of metals as hydrocarbon conversion catalysts is already disputed [16,17], a further inquiry into the subject was conducted.

To this end, the AAEM species content in activated alder char was modified prior to the toluene conversion tests; HCl washing was used to remove the inorganics. In the next step, part of the demineralised batch was impregnated with $Na^+$ ions. As presented in Fig. 13, most of the metals that were originally present in the alder char (AA) were removed by the washing (AA_HCl). After the addition of sodium (AA_Na), the concentration of this element was over 10 times higher than that in the untreated sample.

30 min pyrolytic tests and TGA oxidation analysis of the modified chars were performed to assess the effect of the AAEM species on toluene conversion and char reactivity, respectively. The results obtained were then compared with that of the original, untreated alder char, as presented in Table 6. The toluene pyrolysis over the char bed was not affected by the observed removal of the metal species or by $Na^+$ spiking – the calculated conversions and the benzene yields for all of the applied catalysts were statistically similar. Therefore, the catalytic effect of the AAEM during heterogeneous conversion of toluene was negligible, compared to the strong influence of these elements on char reactivity, as revealed by the TGA analysis. The kinetic parameters of the char oxidation differed substantially, depending on the pre-treatment that was undertaken. The activation energy of the unmodified material (AA) was 2.6 times lower, compared to the demineralised sample (AA_HCl). After impregnation with $Na^+$, the reactivity of the char
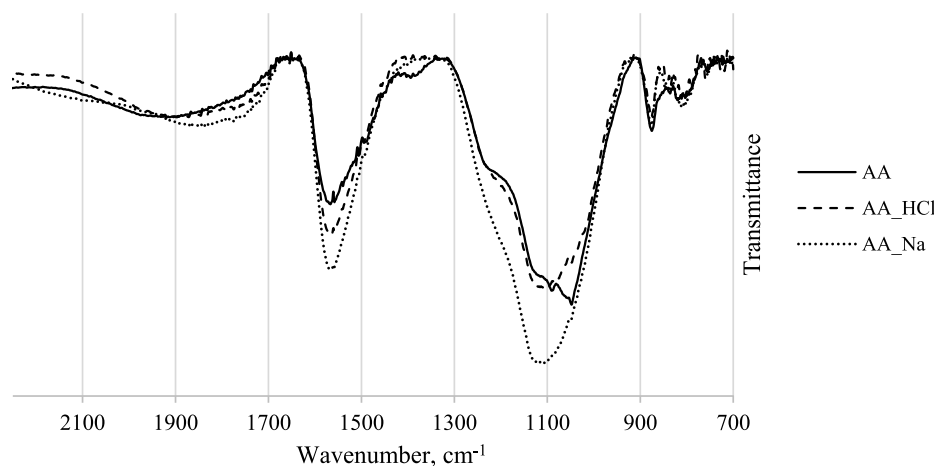
**Fig. 14.** ATR-FTIR spectra of untreated activated alder char (AA), AA char after an HCl wash (AA_HCl) and AA_HCl char after Na$^+$ impregnation (AA_Na).

increased, as indicated by the 30% lower $E_a$ of AA_Na than AA_HCl char. However, oxidation of both modified chars occurred at higher temperatures (peak at 580–590 ℃) compared with the original sample (515 ℃).

It is plausible that some other properties of the char, that are relevant to its catalytic performance and reactivity, were also altered by the pre-treatment. Thus, a $N_2$ adsorption analysis of a sample (AA_Na) after final modifications was carried out. It was established that its surface area had been increased by 5%, however, the share of micropores (61%) remained similar to the initial reading (59%). ATR-FTIR analysis of the washed chars suggested some changes had occurred to their surface chemistry (Fig. 14). The intensity of the spectrum of an acid washed sample did not differ significantly from an original sample. However, the shape of the main absorption regions, representing structural C–C vibrations and various C–O interactions, had been altered. The structures that are responsible for these sharp bands, which are characteristic of the original alder and beech chars, had been removed, possibly due to protonation of some esters, ethers and/or acid anhydrides. The deposition of sodium acetate on the surface of the washed char resulted in increased adsorption in regions of both single and double bonds of carbon with oxygen in the AA_Na spectrum. This development of the surface chemistry could be attributed to acetate ions attaching themselves to the structure of the char, which increased the amount of O-containing functionalities.

## 4. Conclusions

In this paper, pyrolytic conversion of toluene over wood-derived biochars was examined in order to assess their potential for tar removal. Among the three selected tree species that were investigated, coniferous pine yielded char with the highest microporosity, which most likely resulted from its lower oxidation reactivity causing the less pronounced creation of mesopores upon steam activation. Char from pine was also characterized by a lower number of strong acidic sites, which was likely related to the structural differences between raw coniferous and deciduous wood. The less prominent catalytic properties of pine char resulted in it having a worse and more short-term performance as a catalyst for toluene decomposition, compared to the two chars from deciduous trees.

The main experiment of toluene pyrolysis and the additional tests with intermittent feeding revealed the prevalence of heterogeneous decomposition reactions; no gas-phase decomposition of toluene was observed. It was mainly forming coke deposit on the char surface, thus deactivating its catalytic properties. The selectivity towards the competing pathway, leading to benzene and methane formation, increased with the char being saturated with coke, and it reached 12 – 16%.

Secondary reactions of methyl substitution resulted in the creation of small amounts of xylenes and ethylbenzene; the latter underwent intense dehydrogenation to form styrene.

Additional tests with pre-treated activated alder char revealed that while the presence of alkali and alkaline earth metals in the char increased its oxidation rate, it did not affect the efficiency of the pyrolytic conversion of toluene.

## CRediT authorship contribution statement

**Agnieszka Korus:** Conceptualization, Investigation, Writing - original draft, Project administration, Funding acquisition. **Abby Samson:** Supervision, Writing - review & editing. **Andrzej Szlęk:** Supervision, Writing - review & editing.

## Declaration of Competing Interest

The authors declare that they have no known competing financial interests or personal relationships that could have appeared to influence the work reported in this paper.

## Acknowledgements

## References

[1] Ren J, Liu YL, Zhao XY, Cao JP. Biomass thermochemical conversion: a review on tar elimination from biomass catalytic gasification. J Energy Inst 2020;93:1083–98. https://doi.org/10.1016/j.joei.2019.10.003.

[2] Shen Y. Chars as carbonaceous adsorbents/catalysts for tar elimination during biomass pyrolysis or gasification. Renew Sustain Energy Rev 2015;43:281–95. https://doi.org/10.1016/J.RSER.2014.11.061.

[3] Ravenni G, Sárossy Z, Ahrenfeldt J, Henriksen UB. Activity of chars and activated carbons for removal and decomposition of tar model compounds – a review. Renew Sustain Energy Rev 2018;94:1044–56. https://doi.org/10.1016/J.RSER.2018.07.001.

[4] Fuentes-Cano D, von Berg L, Diéguez-Alonso A, Scharler R, Gómez-Barea A, Anca-Couce A. Tar conversion of biomass syngas in a downstream char bed. Fuel Process Technol 2020;199:106271 https://doi.org/10.1016/J.FUPROC.2019.106271.

[5] Fuentes-Cano D, Gómez-Barea A, Nilsson S, Ollero P. Decomposition kinetics of model tar compounds over chars with different internal structure to model hot tar removal in biomass gasification. Chem Eng J 2013;228:1223–33. https://doi.org/10.1016/j.cej.2013.03.130.

[6] Nestler F, Burhenne L, Amtenbrink MJ, Aicher T. Catalytic decomposition of

biomass tars: the impact of wood char surface characteristics on the catalytic performance for naphthalene removal. Fuel Process Technol 2016;145:31–41. https://doi.org/10.1016/j.fuproc.2016.01.020.

[7] Hosokai S, Kumabe K, Ohshita M, Norinaga K, Li CZ, Hayashi J. Mechanism of decomposition of aromatics over charcoal and necessary condition for maintaining its activity. Fuel 2008;87:2914–22. https://doi.org/10.1016/j.fuel.2008.04.019.

[8] Abu El-Rub Z, Bramer EA, Brem G. Experimental comparison of biomass chars with other catalysts for tar reduction. Fuel 2008;87:2243–52. https://doi.org/10.1016/J.FUEL.2008.01.004.

[9] Ravenni G, Elhami OH, Ahrenfeldt J, Henriksen UB, Neubauer Y. Adsorption and decomposition of tar model compounds over the surface of gasification char and active carbon within the temperature range 250–800 °C. Appl Energy 2019;241:139–51. https://doi.org/10.1016/J.APENERGY.2019.03.032.

[10] Bhandari PN, Kumar A, Bellmer DD, Huhnke RL. Synthesis and evaluation of bio-char-derived catalysts for removal of toluene (model tar) from biomass-generated producer gas. Renew Energy 2014;66:346–53. https://doi.org/10.1016/J.RENENE.2013.12.017.

[11] Korus A, Samson A, Szlęk A, Katelbach-Woźniak A, Sładek S. Pyrolytic toluene conversion to benzene and coke over activated carbon in a fixed-bed reactor. Fuel 2017;207. https://doi.org/10.1016/j.fuel.2017.06.088.

[12] Mani S, Kastner JR, Juneja A. Catalytic decomposition of toluene using a biomass derived catalyst. Fuel Process Technol 2013;114:118–25. https://doi.org/10.1016/J.FUPROC.2013.03.015.

[13] Ledesma EB, Campos C, Cranmer DJ, Foytik BL, Ton MN, Dixon EA, et al. Vapor-phase cracking of eugenol: distribution of tar products as functions of temperature and residence time. Energy Fuels 2013;27:868–78. https://doi.org/10.1021/ef3018332.

[14] Lea-Langton AR, Andrews GE, Bartle KD, Jones JM, Williams A. Combustion and pyrolysis reactions of alkylated polycyclic aromatic compounds: the decomposition of 13C methylarenes in relation to diesel engine emissions. Fuel 2015;158:719–24. https://doi.org/10.1016/j.fuel.2015.05.043.

[15] Boehm H, Diehl E, Heck W, Sappok R. Surface oxides of carbon. Angew Chemie Int Ed English 1964;3:669–77.

[16] Klinghoffer NB, Castaldi MJ, Nzihou A. Influence of char composition and in-organics on catalytic activity of char from biomass gasification. Fuel 2015;157:37–47. https://doi.org/10.1016/j.fuel.2015.04.036.

[17] Dufour A, Celzard A, Fierro V, Martin E, Broust F, Zoulalian A. Catalytic decomposition of methane over a wood char concurrently activated by a pyrolysis gas. Appl Catal A Gen 2008;346:164–73. https://doi.org/10.1016/j.apcata.2008.05.023.

[18] Moliner R, Suelves I, Lázaro MJ, Moreno O. Thermocatalytic decomposition of methane over activated carbons: influence of textural properties and surface chemistry. Int J Hydrogen Energy 2005;30:293–300. https://doi.org/10.1016/j.ijhydene.2004.03.035.

[19] Mohamed AR, Mohammadi M, Darzi GN. Preparation of carbon molecular sieve from lignocellulosic biomass: a review. Renew Sustain Energy Rev 2010;14:1591–9. https://doi.org/10.1016/j.rser.2010.01.024.

[20] Molina-Sabio M, Gonzalez MT, Rodriguez-Reinoso F, Sepúlveda-Escribano A. Effect of steam and carbon dioxide activation in the micropore size distribution of acti-vated carbon. Carbon N Y 1996;34:505–9. https://doi.org/10.1016/0008-6223(96)00006-1.

[21] Huang Y, Yin X, Wu C, Wang C, Xie J, Zhou Z, et al. Effects of metal catalysts on CO2 gasification reactivity of biomass char. Biotechnol Adv 2009;27:568–72. https://doi.org/10.1016/j.biotechadv.2009.04.013.

[22] Zhang Z, Pang S, Levi T. Influence of AAEM species in coal and biomass on steam co-gasification of chars of blended coal and biomass. Renew Energy 2017;101:356–63. https://doi.org/10.1016/J.RENENE.2016.08.070.

[23] The Wood Database n.d. https://www.wood-database.com/.

[24] Goertzen SL, Thériault KD, Oickle AM, Tarasuk AC, Andreas HA. Standardization of the Boehm titration. Part I. CO2 expulsion and endpoint determination. Carbon N Y 2010;48:1252–61. https://doi.org/10.1016/j.carbon.2009.11.050.

[25] Oickle AM, Goertzen SL, Hopper KR, Abdalla YO, Andreas HA. Standardization of the Boehm titration: Part II. Method of agitation, effect of filtering and dilute titrant. Carbon N Y 2010;48:3313–22. https://doi.org/10.1016/j.carbon.2010.05.004.

[26] Tsechansky L, Graber ER. Methodological limitations to determining acidic groups at biochar surfaces via the Boehm titration. Carbon N Y 2014;66:730–3. https://doi.org/10.1016/j.carbon.2013.09.044.

[27] Korus A, Szlęk A, Samson A. Physicochemical properties of biochars prepared from raw and acetone-extracted pine wood. Fuel Process Technol 2019;185:106–16. https://doi.org/10.1016/J.FUPROC.2018.12.004.

[28] Feng D, Zhao Y, Zhang Y, Sun S, Meng S, Guo Y, et al. Effects of K and Ca on reforming of model tar compounds with pyrolysis biochars under H2O or CO2. Chem Eng J 2016;306:422–32. https://doi.org/10.1016/J.CEJ.2016.07.065.

[29] Senum GI, Yang RT. Rational approximations of the integral of the Arrhenius function. J Therm Anal 1977;11:445–7. https://doi.org/10.1007/BF01903696.

[30] Delgado JMPQ. A critical review of dispersion in packed beds. Heat Mass Transf 2006;42:279–310. https://doi.org/10.1007/s00231-005-0019-0.

[31] Jess A. Mechanisms and kinetics of thermal reactions of aromatic hydrocarbons from pyrolysis of solid fuels. Fuel 1996;75:1441–8. https://doi.org/10.1016/0016-2361(96)00136-6.

[32] Burhenne L, Damiani M, Aicher T. Effect of feedstock water content and pyrolysis temperature on the structure and reactivity of spruce wood char produced in fixed bed pyrolysis. Fuel 2013;107:836–47. https://doi.org/10.1016/j.fuel.2013.01.033.

[33] Rana R, Langenfeld-Heyser R, Finkeldey R, Polle A. FTIR spectroscopy, chemical and histochemical characterisation of wood and lignin of five tropical timber wood species of the family of Dipterocarpaceae. Wood Sci Technol 2010;44:225–42. https://doi.org/10.1007/s00226-009-0281-2.

[34] Wang S, Wang K, Liu Q, Gu Y, Luo Z, Cen K, et al. Comparison of the pyrolysis behavior of lignins from different tree species. Biotechnol Adv 2009;27:562–7. https://doi.org/10.1016/j.biotechadv.2009.04.010.

[35] Rodrigues J, Faix O, Pereira H. Determination of lignin content of Eucalyptus glo-bulus wood using FTIR spectroscopy. Holzforschung-Int J Biol Chem Phys Technol Wood 1998;52:46–50.

[36] Sjöström E, Alén R, editors. Analytical Methods in Wood Chemistry, Pulping, and Papermaking. first ed. Berlin, Heidelberg: Springer; 1999.

[37] Zieliński W, Rajca A. Metody spektroskopowe i ich zastosowanie do identyfikacji związków organicznych. second ed. Warsaw: Wydawnictwa Naukowo-Techniczne; 2000.

[38] Silverstein RM, Webster FX, Kiemle DJ. Spektroskopowe metody identyfikacji związków organicznych. second ed. Warsaw: Wydawnictwo Naukowe PWN; 2007.

[39] Boehm HP. Some aspects of the surface chemistry of carbon blacks and other car-bons. Carbon N Y 1994;32:759–69. https://doi.org/10.1016/0008-6223(94)90031-0.

[40] Szymański GS, Karpiński Z, Biniak S, Świątkowski A. The effect of the gradual thermal decomposition of surface oxygen species on the chemical and catalytic properties of oxidized activated carbon. Carbon N Y 2002;40:2627–39. https://doi.org/10.1016/S0008-6223(02)00188-4.

[41] Serp P, Figueiredo JL. Carbon materials for catalysis. John Wiley & Sons; 2009.

[42] Figueiredo J, Pereira MF, Freitas MM, Órfão JJ. Modification of the surface chemistry of activated carbons. Carbon N Y 1999;37:1379–89. https://doi.org/10.1016/S0008-6223(98)00333-9.

[43] Zielke U, Hüttinger KJ, Hoffman WP. Surface-oxidized carbon fibers: I. Surface structure and chemistry. Carbon N Y 1996;34:983–98. https://doi.org/10.1016/0008-6223(96)00032-2.

[44] Boudou JP. Surface chemistry of a viscose-based activated carbon cloth modified by treatment with ammonia and steam. Carbon N Y 2003;41:1955–63. https://doi.org/10.1016/S0008-6223(03)00182-9.

[45] Haydar S, Moreno-Castilla C, Ferro-García MA, Carrasco-Marín F, Rivera-Utrilla J, Perrard A, et al. Regularities in the temperature-programmed desorption spectra of CO2 and CO from activated carbons. Carbon N Y 2000;38:1297–308. doi: 10.1016/S0008-6223(99)00256-0.

[46] Tancredi N, Cordero T, Rodríguez-Mirasol J, Rodríguez JJ. Activated carbons from Uruguayan eucalyptus wood. Fuel 1996;75:1701–6. https://doi.org/10.1016/S0016-2361(96)00168-8.

[47] Leininger J-P, Lorant F, Minot C, Behar F. Mechanisms of 1-methylnaphthalene pyrolysis in a batch reactor. Energy Fuels 2006;20:2518–30. https://doi.org/10.1021/ef0600964.